JOURNAL OF MATERIALS SCIENCE **39** (2004) 4451–4457

# Electrochemical growth of aligned N-chiral alkyl substituted polypyrrole micro-ribbons

GAOYI HAN
*Department of Chemistry, Tsinghua University, Beijing 100084, People's Republic of China; Institute of Molecular Science, Shanxi University, Taiyuan 030006, People's Republic of China*

GAOQUAN SHI, JINYING YUAN, FENG'EN CHEN
*Department of Chemistry, Tsinghua University, Beijing 100084, People's Republic of China*
*E-mail: gshi@tsinghua.edu.cn*

Aligned micro-ribbons of N-chiral alkyl substituted polypyrrole have been grown for the first time by electrochemical polymerization of methyl (S)-(+)-2-(1H-pyrrol-yl) propionate (1) and methyl (S)-(−)-3-phenyl-2-(1H-pyrrol-yl) propionate (2) in acetonitrile containing tetrabutylammonium perchlorate ($TBAClO_4$) and camphor-10-sulfonic acid (CSA) enantiomer. The micro-ribbons stand upright on the working electrode surface in a high density. They have a length of 100–200 $\mu$m, a width of 20–50 $\mu$m and a thickness of 3–5 $\mu$m. Scanning electron microscopic (SEM) studies showed that the micro-ribbons were assembled by nanometer balls with diameters of 30–50 nm. A hole growing mechanism was suggested according to the SEM pictures recorded during the electrochemical growth process. The structures of the resulting polymers have been characterized by infrared and Raman spectroscopies. 

## 1. Introduction

Micro- and nano-structured conducting polymeric (CP) materials have attracted increasing attention, mainly due to their potential applications in catalysis, optics, drug delivery and microelectronics [1–3]. Recently, various synthesis methods, including template synthesis, clarity reaction, molecular deposition and electrochemical polymerization with a scanning micro-needle electrode have been developed for synthesis of micro- and nano-structured CPs [4–11]. Among these methods, template synthesis is an effective technique to prepare nanotubes, molecular wires and microballs, and it has been successfully applied to synthesize polyacetylene, polythiophene, polypyrrole and polyaniline [4–7]. Porous structured and nanowires of polypyrrole also have been described in previous literatures [12–14]. On the other hand, chiral conducting polymers are of considerable interest in view of their potential applications as electrodes for electrochemical asymmetric synthesis, stereoselective analysis and chiral stationary phases for the chromatograghic separation of enantiomers [15, 16]. Various chiral pyrrole derivatives with chiral center at least two carbon atoms far from the aromatic rings have been synthesized and polymerized. Salmon and Bidan [17, 18] introduced (S)-(+)-CSA with an alkyl spacer as chiral group at N-position of pyrrole, and the optical activity of the chiral monomer and its polymer was measured by using circular dichromism (CD) spectroscopy. The chiral pyrrole derivatives bring an optical active amide group at 3-position of pyrrole ring and (1S)-(+)-N-(1-phenyletheyl)pyrrole, (1R)-(−)-N-(1-phenylethyl) pyrrole were also synthesized and electropolymerized [19]. Pleus *et al.* [15, 16] reported the electrochemical polymerization of the chiral pyrrole monomers containing (−)-ethyl L-lactate as the chiral functional group either at N- or 3-position of pyrrole. The properties of the polymer as enantioselective electrodes were also investigated. Polypyrroles with amino acids substituted group have chirality in their main chain because of an asymmetric induction originating from the chiral substituents [20]. The present paper reports the results of electrochemical polymerization of two N-chiral alkyl substituted pyrrole derivatives with chiral carbon connected to the N atom of the pyrrole rings. Surprisingly, well aligned micro-ribbons of the polymers were generated.

## 2. Experimental section

### 2.1. Materials

(S)-(+)-CSA and (R)-(−)-CSA were purchased from Fluka and used as received. 2, 5-dimethoxytetrahydrofuran (Acros 99%) was also used without further purification. The pyrrole derivatives of methyl (S)-(+)-2-(1H-pyrrol-yl) propionate (**1**), methyl (S)-(−)-3-phenyl-2-(1H-pyrrol-yl) propionate (**2**) and methyl (1H-pyrrol-yl) acetate (**3**) (Scheme 1) were synthesized in our lab according to a literature method [21, 22]. All other chemicals were reagent grade. Acetonitrile was purified through the published procedures [23]. $TBAClO_4$ was dried under vacuum at 80°C for 12 h before use.

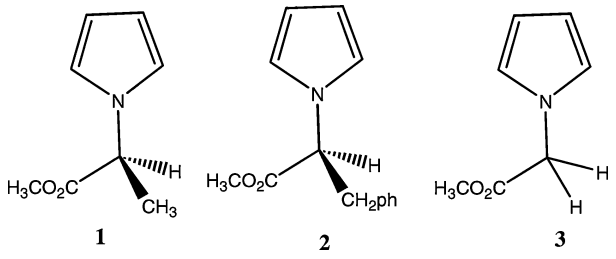


*Scheme 1*

## 2.2. Polymer preparation and characterization

The growth of microstructures was carried out at room temperature in a single compartment cell by the use of a Model 283 potentiostat-galvanostat (EG&G Princeton Applied Research) under computer control. The working and counter electrodes were two platinum sheets with surface areas of 0.5 $cm^2$ and 1.0 $cm^2$, respectively, and placed 1.0 cm apart. All potentials were referred to a saturated calomel electrode (SCE). The solutions were degassed by dry nitrogen bubbling and maintained at a light overpressure during the experiments. The typical electrolyte was the acetonitrile solution of 0.1 M pyrrole derivative, 0.1 M $TBAClO_4$ and 0.1 M (S)-(+)-CSA or (R)-(−)-CSA.

Optical rotations of the monomer were measured by means of a WZZ-ZA automatic polarimeter. The infrared spectra were obtained by the use of a Spectrum GX FT-infrared spectrometer of Perkin-Elmer Company. Raman spectra were recorded by using a RM 2000 microscopic confocal Raman spectrometer (Renishaw PLC, England) employing a 633 nm laser beam at 0.1 mW and a charge couple device (CCD) detector with 4 $cm^{-1}$ resolution. The spectrum was accumulated 3 times for 50 s each. The morphology of the microstructures was studied using a KYKY2800 scanning electron microscopy (SEM) after spurtter-coating the samples with gold and field-emitting SEM (JSE-6700F, Jeol) after spurtter-coating with platinum. XPS data were recorded by using a PHI5300 ESCA/610SAM spectrometer under the pressure lower than $10^{-8}$ torr. The conductivity of the polymers was measured by the conventional four-probe technique and using the pressed discs of the polymers as the samples.

## 3. Results and discussion

### 3.1. Electrochemical polymerization

The polymerization rates of monomers **1**–**3** in acetonitrile containing only (S)-(+)-CSA or (R)-(−)-CSA are fairly low. In order to get a sensible film in a reasonable time period, a certain amount of $TBAClO_4$ was added into the medium to increase the ionic conductivity of the electrolyte and accelerate the reaction. Fig. 1 shows the successive cyclic voltammograms (CV) of 0.1 M monomer in acetonitrile containing 0.1 M $TBAClO_4$ and 0.1 M (R)-(−)-CSA or (S)-(+)-CSA. During the process of CV scanning, the color of the solution near to the working electrode surface changed from transparent to brown because part of the monomer was oxidized into oligomers, which were dissolved or dispersed into the solution. Each CV showed a couple of broad redox waves (Fig. 1a, b, d) of the polymer in the potential range of 0.3–1.0 V. The strong oxidation current wall appeared at the potentials higher than ca. 1.0 V led to the formation of a black film on the working electrode surface. The increase of the redox wave currents of the polymer implied that the amount of the polymer on the electrode was increased. However, in the case of electrolysis of **2**, no polymer film was formed on the electrode surface during the process of successive cyclic voltammetric scanning. The redox waves of the polymer were also not observed in Fig. 1c. This is mainly due to that the large graft chain of **2** increased the solubility of the polymer in the reduced state. Therefore, the polymer was dissolved into the electrolyte at low potentials. Fortunately, the polymer in the oxidized state is insoluble, and the polymer film can be generated by electrolysis at constant potentials.

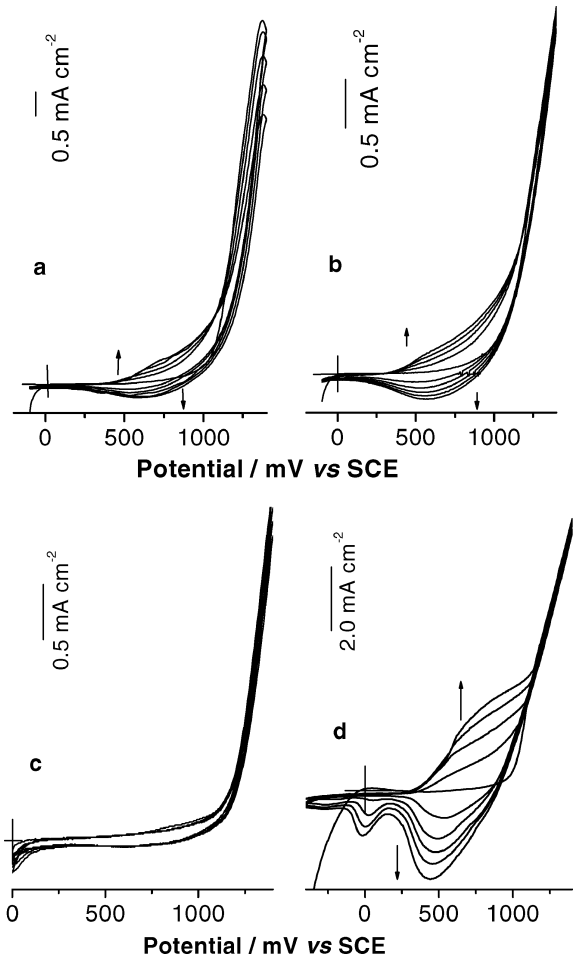


*Figure 1* Successive CVs of 0.1 M monomer **1** in acetonitrile solution of 0.1 M $TBAClO_4$ + 0.1 M (S)-(+)-CSA (a) or 0.1 M $TBAClO_4$ + (R)-(−)-CSA (b); 0.1 M **2** in acetonitrile solution of 0.1 M $TBAClO_4$ + 0.1 M (R)-(−)-CSA (c) and 0.1 M **3** in acetonitrile solution of 0.1 M $TBAClO_4$ + 0.1 M (S)-(+)-CSA (d) at a potential scan rate of 50 mV $s^{-1}$.

### 3.2. Morphology

Fig. 2A illustrates a typical scanning electron micrograph of the polypyrrole micro-ribbons formed by electrolysis of 0.1 M monomer **1**, a positive optical rotation monomer potentiostatically at 1.4 V for 4000 s in the medium containing 0.1 M $TBAClO_4$ and 0.1 M

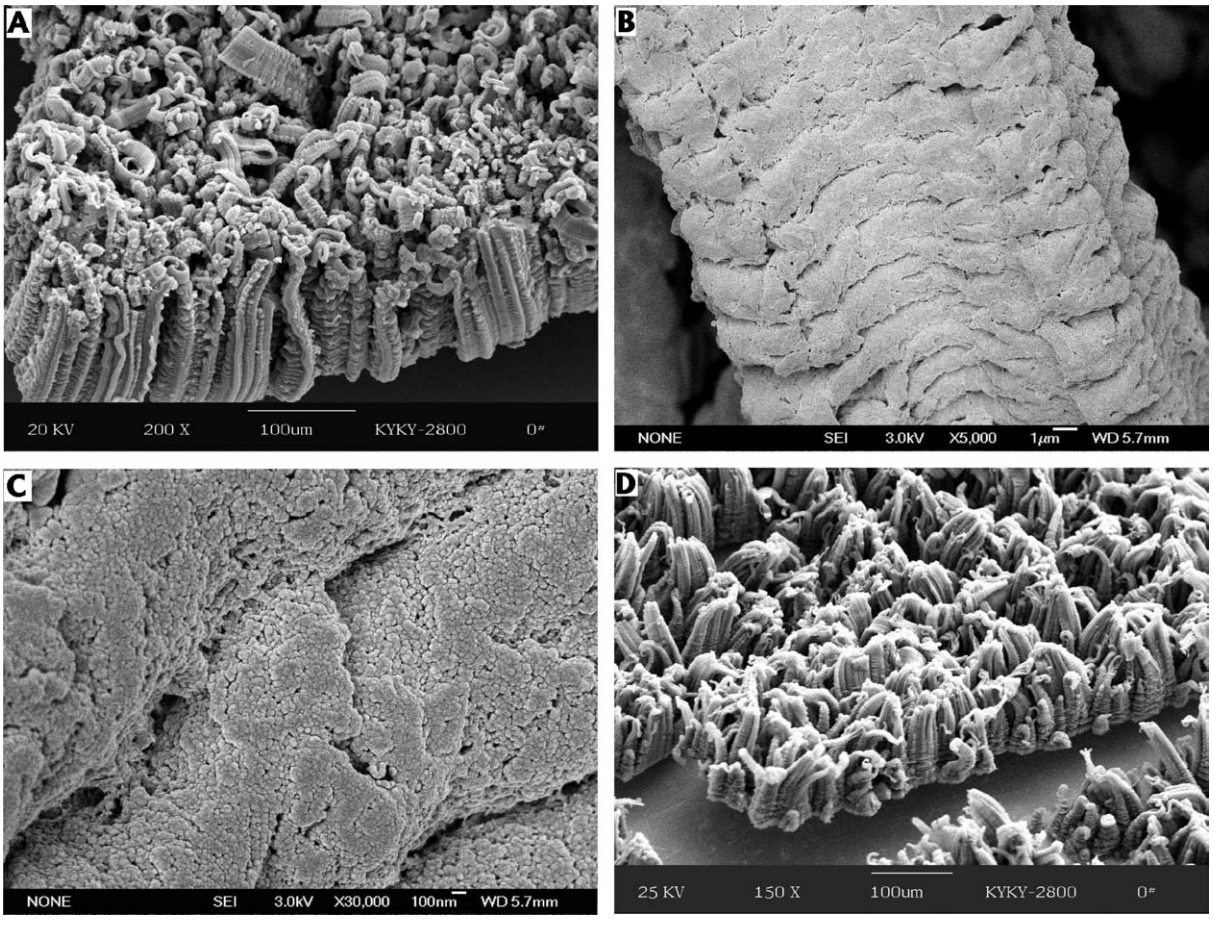


*Figure 2* SEM images of the aligned micro-ribbons prepared by electrosynthesis of 0.1 M monomer **1** in acetonitrile containing 0.1 M $TBAClO_4$ and 0.1 M (S)-(+)-CSA (A) at 1.4 V for 4000 s or at a constant current density of 4 mA $cm^{-2}$ for 1000 s (D); (B) and (C) are magnified views of a single micro-ribbon in Fig. 2A.

(S)-(+)-CSA (similar morphology was also observed at 1.3 V). It is clear from this figure that the micro-ribbons stand upright on the electrode surface. The micro-ribbons have a fairly good uniformity and aligned in a high density. A single ribbon has a size of 100–200 $\mu$m in length, 20–50 $\mu$m in width and 3–5 $\mu$m in thickness. The magnified view of a single micro-ribbon (Fig. 2B) demonstrates that the micro-ribbons are made of stacked blocks of polymer film with 2–3 $\mu$m in height and 8–10 $\mu$m in width. Higher resolution SEM images of the polymer blocks indicate that micro-ribbons were assembled by nano-balls with diameters of 30–50 nm (Fig. 2C). In the same medium, the micro-ribbons also can be grown by electrolysis of 1 at a constant current density in the scale of 2–4 mA $cm^{-2}$. A typical morphology of the aligned micro-ribbons is shown in Fig. 2D.

In the medium without CSA, high quality micro-ribbons can not be generated (Fig. 3A). On the other hand, when (R)-(−)-CSA was used as one of the

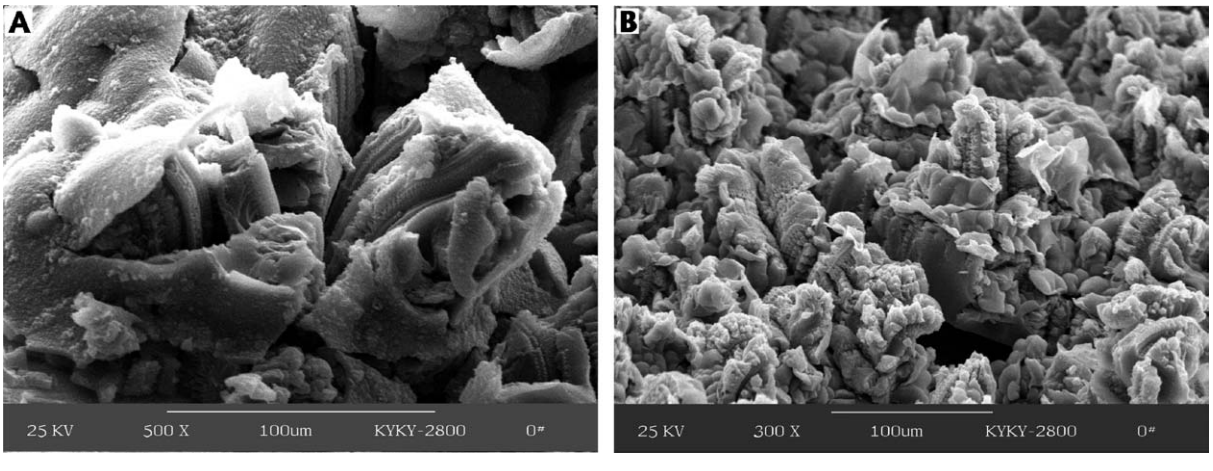


*Figure 3* SEM images of the micro-ribbons prepared by electrosynthesis of 0.1 M monomer **1** at 1.4 V in acetonitrile containing 0.1 M $TBAClO_4$ for 4000 s (A); or in acetonitrile containing 0.1 M $TBAClO_4$ and 0.1 M (R)-(−)-CSA for 4000 s (B).

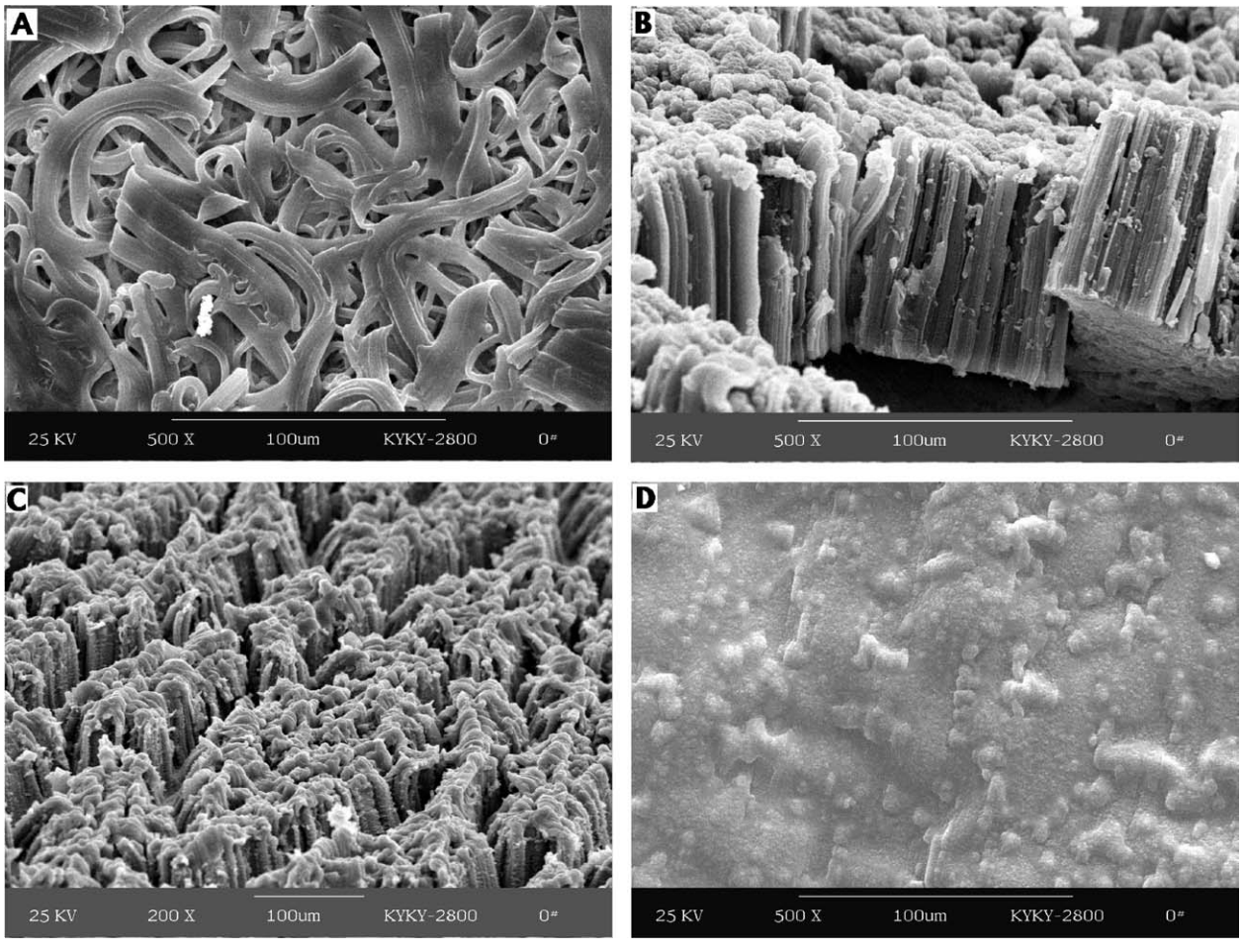


*Figure 4* SEM images of the micro-ribbons prepared by electrosynthesis of 0.1 M monomer **2** in acetonitrile containing 0.1 M $TBAClO_4$ and 0.1 M (R)-(−)-CSA at 1.4 V for 6500 s (A); or at 1.5 V for 3500 s (B); or in acetonitrile containing only 0.1 M $TBAClO_4$ at 1.5 V for 4000 s (C); and a film formed by electrolysis of 0.1 M monomer **3** in acetonitrile containing 0.1 M $TBAClO_4$ and 0.1 M (S)-(+)-CSA at 1.4 V for 4000 s (D).

supporting electrolytes, the aligned micro-ribbons can be grown in a low density. However, they are much shorter than those in Fig. 1A. X-ray photoelectron spectroscopy analysis results indicated that the doping levels of the polymer obtained from the system with (S)-(+)-CSA (polymer A) or (R)-(−)-CSA (polymer B) are almost the same (∼16%) from the atomic ratio of $(n_{Cl} + n_S)/n_N$ (where $n_{Cl}$, $n_S$ and $n_N$ are the atomic contents of Cl, S and N in the polymers, respectively). However, the CSA content of polymer A ($n_S/n_N \sim 0.16$) is almost two times that of polymer B ($n_S/n_N \sim 0.077$). This implied that the co-deposition of CSA had contributions to the formation of aligned micro-ribbons.

Micro-ribbons can also be prepared by electrolysis of **2**, a negative optical rotation monomer in the media containing (R)-(−)-CSA and $TBAClO_4$ (Fig. 4A and B) or only $TBAClO_4$ (Fig. 4C). As show in Fig. 4A the micro-ribbons grown at a constant potential of 1.4 V are tortuous on the surface of working electrode. However, at an applied potential of 1.5 V, the micro-ribbons are standup right on the surface of the electrode in a high density. The ribbons are straight and have smooth surfaces. In contrast, in the medium containing (S)-(+)-CSA, no micro-ribbons were formed because the as-formed polymer was dissolved or dispersed into the solution. Monomer **3** does not bring a chiral carbon and the size of the graft chain is smaller than those of **1** and **2**. As a result, electrolysis of **3** generated a compact thin film, and no micro-ribbon was obtained (Fig. 4D).

### 3.3. Infrared and Raman spectra

Fig. 5A shows the transmission IR spectra of the polymers synthesized from monomer **1**. It is clear from this figure that these two samples have similar chemical structures. The weak peak at 3127 $cm^{-1}$ is assigned to the ring C─H stretching of pyrrole rings. The peaks at 2950 and 2876 $cm^{-1}$ are attributed to the asymmetric and symmetric methyl C─H stretching. The very strong peak at 1741 $cm^{-1}$ is due to the stretching of carbonyl groups; 1554 $cm^{-1}$ peak is assigned to the ring C═C vibration; bands at 1472, 1435 and 1379 $cm^{-1}$ are due to C─N vibrations and C─H deformations respectively. Furthermore, the band at 1209 $cm^{-1}$ is due to stretching of ─COOR group and doping agent R-$SO_3^-$, and the band at 1086 $cm^{-1}$ is assigned to the doped $ClO_4^-$ and the C─O stretching mode. Bands at 849, 740 and 623 $cm^{-1}$ may be belong to C─H deformations and $CH_3$ rocking [24, 25]. The spectral results described above confirmed that the micro-ribbons are made of N-alkyl substituted polypyrrole in the oxidized (doped) state.

Fig. 5B shows the typical Raman and polarized Raman spectra of the polymer synthesized from monomer **1**. The 1742 $cm^{-1}$ band is assigned to the

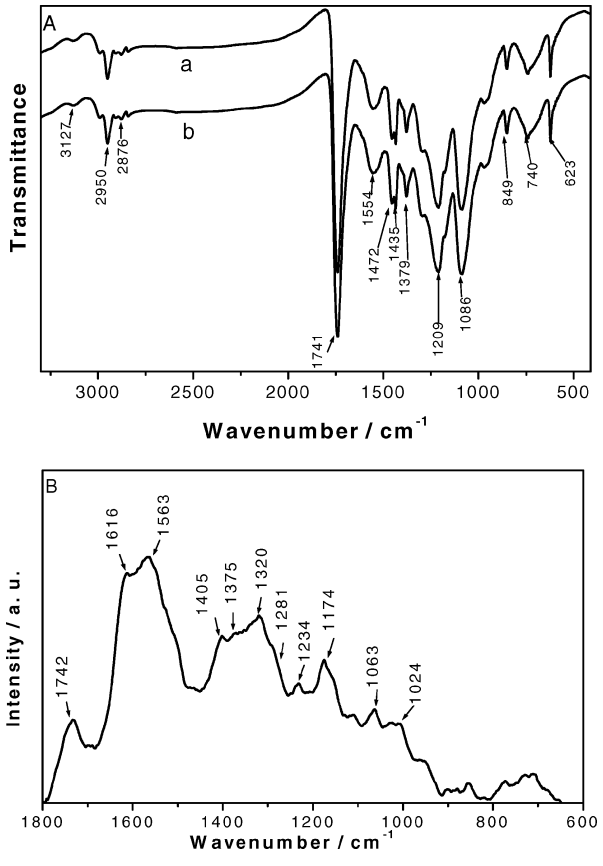


*Figure 5* A: Transmission FT-IR spectra of the micro-ribbons prepared by electrolysis of 0.1 M monomer **1** in acetonitrile containing 0.1 M $TBAClO_4$ and 0.1 M (S)-(+)-CSA (a) or (R)-(−)-CSA (b); B: 633 nm excited Resonance Raman spectrum micro-ribbons prepared by electrolysis of 0.1 M monomer **1** in acetonitrile containing 0.1 M $TBAClO_4$ and 0.1 M (S)-(+)-CSA at 1.4 V for 4000 s.

stretching of carbonyl group. According to the literatures [10, 26–32], the 1616 $cm^{-1}$ band is attributed to the C═C bond stretching of the oxidized species and the band at 1563 $cm^{-1}$ is associated with the C═C stretching of the neutral species. The peaks at *ca.* 1320 $cm^{-1}$, 1380 $cm^{-1}$ and 1234 $cm^{-1}$ are due to be the rings stretching mode of polypyrrole. The peak at 1281 $cm^{-1}$ is regarded as C─C stretching between the rings. The band at 1174 $cm^{-1}$ is assigned to the R-$SO_3^-$ symmetric stretching of the doping agent. The peaks ranged from 1000 to 1150 $cm^{-1}$ are originated from ring C–H deformations. The Raman results strongly support the conclusion derived from the infrared spectra described above.

## 3.4. Formation mechanism

Fig. 6 presents the SEM images of polymer coated electrode surface recorded at different polymerization time. It is clear from Fig. 6A, a smooth thin polypyrrole film was formed on the working electrode surface in the initial period of polymerization. With the increase of the polymerization time, the film was cracked by the successively generated polymer particles under the film. Then the clusters of polymer particles grew out from the micro-crazes (Fig. 6B), and the clusters grew longer and longer gradually and assembled into aligned micro-ribbons (Fig. 6C and D).

The chronoamperograms of electrochemical polymerization of monomer **1**–**3** on the platinum electrode are shown in Fig. 7. As can be seen from this figure, a significant decrease in current density was found in the initial stage. This is mainly due to an instantaneous nucleation process with three-dimensional growth on the electrode surface [33]. When a polymer film was formed, the monomer diffused to the electrode surface through the micro-holes of the film and the current density increased until it reached a plateau value for **1** or **2** (Fig. 7a and b). During this period, polypyrrole ribbon was produced. The slight current vibration is resulted from polymer chain arrangement and changes in electrode surface area. However, for monomer **3** (Fig. 7c), polymerization did not result in the formation of micro-ribbons, and the current density decreased until it reached a plateau value close to zero. This result implied that the polymer film gradually stopped growing in the case of electrolysis of monomer **3**.

Accordingly, we can conclude that the growth mechanism of polypyrrole ribbons in this system is different from that of fabrication of conducting polymer microstructures by electropolymerization in porous membranes [34]. In template synthesis, conducting polymer starts to grow from the electrode surface, and the microstructures grow long by deposition of polymer on the surface of the film. This route is possible only in the case of conducting polymers having high conductivity. In contrast, as described above, the micro-ribbons are grown at the bottom like the growth of a tree. The polymers made from **1** and **2** have bulky chiral graft chains. This weaken the inter chain interactions and favored to form a loosely piled porous film. The co-deposition of the large anions of CSA also supports the formation of this film morphology. On the other hand, the conductivity of the polymers prepared from the N-substituted pyrrole derivatives **1**–**3** are fairly low, in the order of $10^{-6}$–$10^{-5}$ S $cm^{-1}$. Therefore, accompany with the increase of film thickness, the resistance of the film increase and which resulting in large iR drop during the polymerization. This finally prevents the monomer to be polymerized on the surface of the film. In the systems with **1** and **2**, the monomers can diffuse to the electrode surface through the loosely piled porous films and the polymers can grow under the film successively. The newly formed polymer nanoparticles stacked into micro-clusters, and penetrated out the film. The micro-clusters preserved horizontal growth at their roots to form micro-ribbons. In contrast, electrolysis of **3** resulted in the formation of a compact film mainly due to the graft chain of the monomer is straight and relatively small. Thus, the polymerization can not be carried out under the film and no micro-ribbons formed in any cases. It also should be noted here that as the structure of the chiral CSA anion matches the polymer structure ((S)-(+)-CSA for the polymer made from **1**, and (R)-(−)-CSA for polymer made from **2**) the anion can be co-deposited into the film to a high content and which supports the formation of micro-ribbons as described above. Otherwise, it is impossible to grow micro-ribbons with high quality.

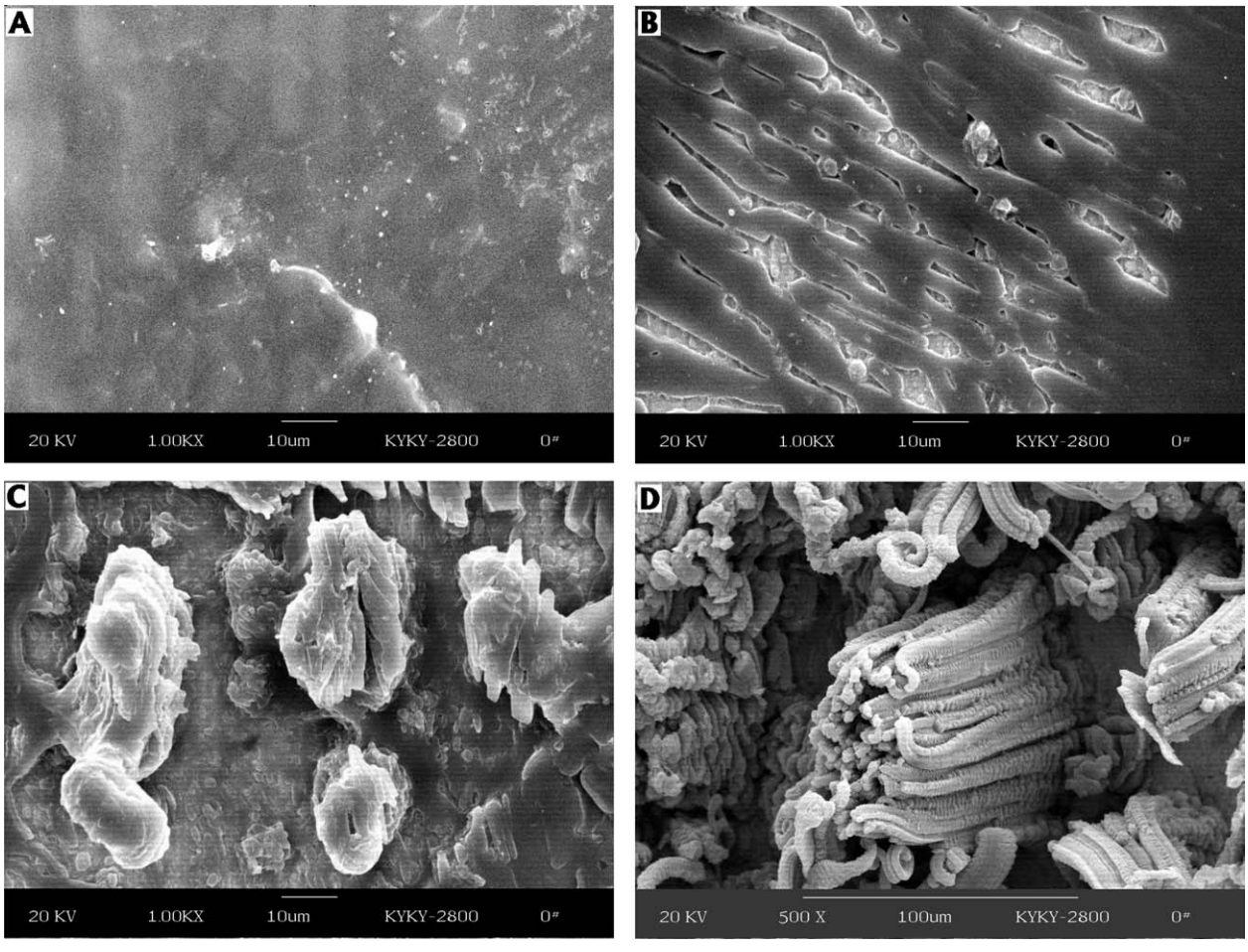


*Figure 6* SEM images of the PPy micro-ribbons grown in the medium of acetonitrile containing 0.1 M monomer **1**, 0.1 M $TBAClO_4$ and 0.1 M (S)-(+)-CSA at a constant potential of 1.4 V for 300 (A), 1000 (B), 1700 (C), 3000 s (D), respectively.

## 4. Summary

Aligned micro-ribbons of N-chiral alkyl substituted polypyrrole can be electro-synthesized by direct oxidation of monomer **1** and **2**. The morphology of micro-ribbons depends strongly on the monomer structures and chiral environment. The bulky N-substituted chiral graft chains of **1** and **2** lead the formation of porous and loosely piled film with low conductivity. This prevents the formation of thick polymer films and forces the monomer diffuse to the electrode surface and polymerized under the film. The polymer particles under the film assembled to clusters, which penetrated out from the crazes of the film and kept grown into micro-ribbons.

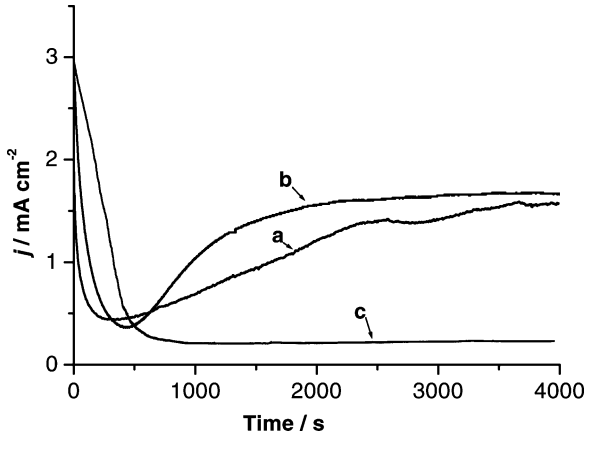


*Figure 7* Chronoamperograms recorded during the electrolysis process of 0.1 M monomer **1** in acetonitrile containing 0.1 M $TBAClO_4$ + 0.1 M (S)-(+)-CSA (a); 0.1 M **2** in acetonitrile containing 0.1 M $TBAClO_4$ + 0.1 M (R)-(−)-CSA (b) and 0.1 M **3** in acetonitrile containing 0.1 M $TBAClO_4$ + 0.1 M (S)-(+)-CSA (c) at 1.4 V.


## Acknowledgements

We thank the National Science Foundation of China for support of this work (Nos. 50225311, 50133010, 50073012).


## References


1. R. POOL, *Science* **247** (1990) 1410.
2. M. X. WAN, J. HUANG and Y. Q. SHEN, *Synth. Met.* **101** (1999) 708.
3. C. R. MARTIN, *Science.* **266** (1994) 1961.
4. Z. CAI and C. R. MARTIN, *J. Amer. Chem. Soc.* **111** (1989) 4138.
5. R. V. PARTHASARATHY and C. R. MARTIN, *Chem. Mater.* **6** (1994) 1627.
6. J. MANSOURI and R. P. BURFORD, *J. Membr. Sci.* **87** (1994) 23.
7. Z. X. WEI and M. X. WAN, *Adv. Mater.* **14** (2002) 1314.
8. S. S. SHIHIRATORI, S. MORI and K. IKEZAKI, *Sens. Actuators* B **49** (1998) 30.
9. M. DELVAUX, J. DUCHET, P.-Y. STAVAUX, R. LEGRAS and S. DEMOUSTIER-CHAMPAGNE, *Synth. Met.* **113** (2000) 275.

10. J. DUCHET, R. LEGRAS and S. DEMOUSTIER-CHAMPAGNE, *ibid.* **98** (1998) 113.
11. S. J. CHEN, D. Y. WANG, C. W. YUAN, X. D. WANG, P. Y. ZHANG and X. S. GU, *J. Mater. Sci. Lett.* **19** (2000) 2157.
12. C. JEROME, D. LABAYE, I. BODART and R. JEROME, *Synth. Met.* **101** (1999) 3.
13. C. JEROME and R. JEROME, *Angew. Chem. Int. Ed.* **37** (1998) 2488.
14. G. A. OZIN, *Adv. Mater.* **4** (1992) 612.
15. S. PLEUS and B. SCHULTE, *J. Solid State Electrochem.* **5** (2001) 522.
16. S. PLEUS and M. SCHWIENTEK, *Synth. Met.* **95** (1998) 233.
17. M. SALMON and G. J. BIDAN, *Electrochem. Soc.* **132** (1985) 1897.
18. M. SALMON, M. SALOMA, G. BIDAN and E. M. GENIES, *Electrochim. Acta.* **14** (1989) 117.
19. F. CHEN, P. AKHTAR, L. A. P. KANE-MAGUIRE and G. G. WALLACE, *Aust. J. Chem.* **50** (1997) 39.
20. D. DELABOUGLISE and F. GARNIER, *Synth. Met.* **39** (1990) 117.
21. T. J. BOND, R. JENKINS, A. C. RIDLEY and P. C. TAYLOR, *J. Chem. Soc. Perkin Trans.* **1** (1993) 2241.
22. M. C. CORVO and M. M. A. PEREIRA, *Tetrahedron Let.* **43** (2002) 455.
23. M. WALTER and L. RAMALEY, *Anal. Chem.* **45** (1973) 165.
24. E. LARRAZ, M. I. REDONDO, M. J. GONZALEZ-TEJERA, M. A. RASO, J. TORTAJADA, DE LA E. S. BLANCA and M. V. GARCIA, *Synth. Met.* **122** (2001) 413.
25. M. I. REDONDO, E. S. DE LA BLANCA, M. V. GARCIA, M. A. RASO, J. TORTAJADA and M. J. GONZALEZ-TEJERA, *ibid.* **122** (2001) 431.
26. Y. C. LIU, B. J. HWANG, W. J. JIAN and R. SANTHANAM, *Thin. Solid. Film.* **374** (2000) 85.
27. Y. C. LIU and B. J. HWANG, *Synth. Met.* **113** (2000) 203.
28. A. J. G. ZARBIN, M.-A. DE PAOLI and O. L. ALVES, *ibid.* **99** (1999) 227.
29. Y. FUKUKAWA, S. TAZAWA, Y. FUJII and I. HARADA, *ibid.* **24** (1988) 329.
30. C. M. JENDEN, R. G. DAVIDSON and T. G. TURNER, *Polymer.* **34** (1993) 1649.
31. C. J. ZHONG, C. Q. TIAN and Z. W. TIAN, *J. Phys. Chem.* **94** (1990) 113.
32. A. B. GONÇALVES, A. S. MANGRICH and A. J. G. ZARBIN, *Synth. Met.* **114** (2000) 119.
33. S. ASAVAPIRIYANONT, G. K. CHANDLER, G. A. GUNAWARDENA and D. PLETCHER, *J. Electroana. Chem.* **177** (1984) 229.
34. S. DEMOUSTIER-CHAMPAGNE, E. FERAIN, C. JEROME, R. JEROME and R. LEGRAS, *Eur. Polym. J.* **34** (1998) 1767.

*Received 17 November 2003*
*and accepted 6 April 2004*